Comfort evaluation of prefabricated and assembled pedestrian cable-stayed bridges

Hui Yingxin[1,2] Wang Wenwei[3] Liu Xinnan[3]

([1] School of Civil and Hydraulic Engineering, Ningxia University, Yinchuan 750021, China)
([2] Ningxia Hui Autonomous Region Engineering Technology Research Center for Maintenance, Yinchuan 750004, China)
([3] School of Transportation, Southeast University, Nanjing 211189, China)

Abstract: To study the vibration responses of prefabricated assembled structures, the comfort of a prefabricated assembled pedestrian cable-stayed bridge was evaluated by limiting the acceleration behavior of the structure. The mode shapes and natural frequencies of the structure under ambient excitation were determined by installing acceleration sensors at the control points. According to the structural characteristics of the elastic connection of the bridge deck splicing, the stiffness of the elastic connection between adjacent segments was determined. Pedestrian and vehicle traffic load analysis models were established according to relevant guidelines. The peak acceleration and acceleration limit under pedestrian and vehicle traffic loads were compared, and the comfort degree of the pedestrian cable-stayed bridge was evaluated. The results show that the natural vibration frequency and peak acceleration match well with the measured values. Considering the reduction of the structural stiffness caused by the prefabricated assembly, the vibration characteristics of the prefabricated assembly structure can be truly reflected thereafter. The comfort evaluation index of the prefabricated assembly structure is consistent with that of the integral structure. The coupling effect between the pedestrian load and vehicle traffic load can be significantly ignored. The vehicle traffic load has a certain degree of influence on structural comfort.

Key words: prefabricated assembled pedestrian cable-stayed bridge; elastic connection stiffness; vehicle load; vibration; comfort evaluation

DOI: 10.3969/j.issn.1003 – 7985.2023.01.004

A prefabricated cable-stayed pedestrian bridge is a lightweight and low-damping structure. If not properly designed, it will cause a large vibration response of the structure, especially when the natural vibration frequency of the structure is close to the step frequency of walkers[1]. As a result, pedestrians may feel uncomfortable and even dangerous if the vibration response of the bridge exceeds the limit of human tolerance. For instance, the Millennium Bridge, built on the Thames River in London, had to be closed due to excessive vibrations after three days of opening[2]. In terms of the vibration comfort of pedestrian bridges, several scholars have performed corresponding research works from the aspects of the pedestrian load model, comfort evaluation method, and vibration reduction design[3-9]. Apart from these, to avoid comfort problems when passersby walk on a pedestrian bridge, a series of specifications or standards have been issued. For example, China design specifications[10] required that the vertical natural frequency of the bridge superstructure should be larger than 3 Hz to avoid the resonance of pedestrian bridges. Moreover, using the German standard EN03[11] and British standard BS 5400-2[12], the comfort of pedestrian overpasses is evaluated using the maximum vibration response of a structure under the walking load.

Intensive research has been conducted to find solutions to mitigate the vibration response of bridges and enhance the comfort of walkers. However, compared with monolithic pedestrian bridges, the structural stiffness and natural vibration frequency of prefabricated pedestrian overpasses are changed because of the assembly joints, which means that the existing comfort evaluation method for monolithic pedestrian bridges is probably not suitable for prefabricated ones. However, few publications are available to guide the design and maintenance of prefabricated bridges. To fill this knowledge gap, a prefabricated and assembled cable-stayed pedestrian bridge served as the research reference in this study. In addition, the vibration response of a pedestrian bridge was measured, and the natural vibration frequency and damping ratio of the pedestrian bridge were identified. Moreover, considering the splicing characteristics of the prefabricated assembly structure, the finite element (FE) model of the pedestrian bridge was established, and the determination and modeling of pedestrian and traffic loads were presented. Fur-

Received 2022-08-07, **Revised** 2022-12-11.

Biography: Hui Yingxin (1985—), male, doctor, professor, huiyx@seu.edu.cn.

Foundation item: National Natural Science Foundation of China (No. 51578135, 51878156, 52268077), Postgraduate Research and Practice Innovation Program of Jiangsu Province (No. SJCX17_0042, KYCX18_0126), Key R&D Program of Ningxia Hui Autonomous Region (No. 2022 BEG03062).

Citation: Hui Yingxin, Wang Wenwei, Liu Xinnan. Comfort evaluation of prefabricated and assembled pedestrian cable-stayed bridges[J]. Journal of Southeast University (English Edition), 2023, 39(1): 26 – 32. DOI: 10.3969/j.issn.1003 – 7985.2023.01.004.

thermore, the accuracy of the FE model was validated by comparing the measured and simulated natural vibration frequency and dynamic response of the reference bridge. Finally, an evaluation framework was proposed and utilized to check the comfort of the pedestrian bridge.

1 Modeling of Prefabricated and Assembled Pedestrian Cable-Stayed Bridges

1.1 Bridge introduction

The response of a low-tower cable-stayed pedestrian bridge was investigated in this study. The span of this bridge is 10 m + 34 m + 10 m. The main tower is a round-arch tower column, and the upper part of the main tower, which crosses the bridge syncline obliquely to optimize the inner force in the stay cable, is made of rectangular hollow steel pipes. The substructure is composed of a rectangular pier of concrete-filled steel tubes. A two-way sliding-plate rubber bearing, which has a dimension of 180 mm × 150 mm × 44 mm, was placed on the cross beam of the main tower, and the elastic modulus of the rubber pad was 90 MPa[13]. The stay cable is a steel strand cable, and the spatial arrangement of the stay cables is double-sided fan-shaped. The foundation of each bridge pier is composed of five precast/prestressed concrete hollow piles. Grade C40 concrete was adopted to construct the main girder, and the compressive and tensile strengths of the concrete are 18.4 and 2.39 MPa, respectively. Moreover, the tensile strength of longitudinal reinforcements and stirrup hoops are 280 and 195 MPa, respectively. The overall layout of the bridge is shown in Fig. 1.

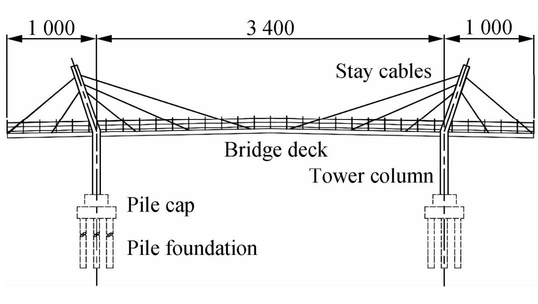

Fig. 1 General layout of the pedestrian footbridge (unit: cm)

The prefabricated and assembled main girder and bridge deck consist of 14 segments, and the adjacent segments were connected by high-strength shear bolts with a joint width of 0.3 m. The height of the girders ranges from 0.45 to 0.55 m, and the thickness of the bridge decks is 0.2 m. Meanwhile, the full width and net width of the bridge deck are 5.06 and 4.00 m, respectively. Furthermore, concrete with a compressive strength of 40 MPa was adopted in this study.

1.2 Finite model of the bridge

FE software midas Civil was utilized to analyze the vibration of the bridge. The main girder, bridge deck, main tower, and bridge piers were modeled with beam elements, and the stay cables were modeled with truss elements. To model the intersection between the soil and pier foundation, equivalent soil springs were applied to nodes belonging to the pile foundation[14]. The bridge deck pavement load was taken as 3.4 kN/m^2, and the pedestrian load was applied in accordance with the German pedestrian bridge design guide EN03[11] and British BS 5400-2 specification[12].

1.3 Modeling of the segment connection

The main girder and bridge deck of the pedestrian bridge were fully prefabricated and assembled, and the adjacent segments were lapped by teeth. High-strength bolts and nuts were employed to connect the adjacent segments, as shown in Fig. 2. This connection method allows the shear force and bending moment to be transmitted. In addition, the bolts and nuts can function smoothly when a large rotation deformation between two adjacent segments occurs. The translation in the longitudinal direction (x direction), vertical (z direction), and rotation in the transverse direction (y direction) were set as elastic connections, and the other three degrees of freedom were set as rigid connections, as shown in Fig. 3.

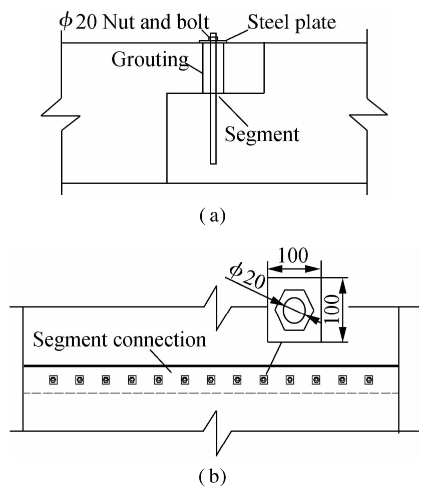

Fig. 2 Bridge deck splicing structure (unit: mm). (a) Horizontal view; (b) Vertical view

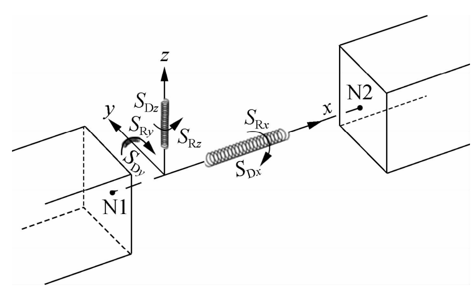

Fig. 3 Diagram of elastic connection parameters

To determine the elastic connection stiffnesses of S_{Dx}, S_{Dz}, and S_{Ry}, the following assumptions were made:

1) Only the constraint effect of the bolts is considered in the segment connection.

2) Plastic properties are not considered while the bolts deform.

3) Under the action of the external load, the segment rotates around point O, as shown in Fig. 4.

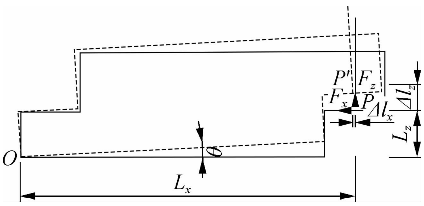

Fig. 4 Segmental deformation diagram

There is a point P at the connection between the bolt and concrete interface. After the relative displacement of the segment, the point reaches P'. Meanwhile, the longitudinal and vertical displacement generated at the connection interface are Δl_x and Δl_z, respectively. The distance from point O to the center line of the bolt is l_x, the vertical distance to the connection interface is l_z, and the length of the bolt is l.

The elastic joint stiffness of S_{Dx} refers to the force required to produce a unit displacement along the x direction, namely,

$$S_{Dx} = n\frac{F_x}{\Delta l_x} = n\frac{G\gamma A}{\Delta l_x} \tag{1}$$

where Δl_x is the longitudinal displacement at the interface connection; F_x is the force required for generating the longitudinal displacement Δl_x; G and E are the shear modulus and elastic modulus of the bolt, respectively; $G = E/[2(1+\mu)]$; γ is the shear strain of the bolt; A and n are the cross-sectional area and the number of bolts, respectively.

The shear strain can be written as

$$\gamma = \frac{\Delta l_x}{l} \tag{2}$$

Combining Eqs. (1) and (2),

$$S_{Dx} = n\frac{GA}{l} \tag{3}$$

The elastic connection stiffness S_{Dz} refers to the force required for generating unit vertical displacement:

$$S_{Dz} = n\frac{F_z}{\Delta l_z} = n\frac{E\varepsilon A}{\Delta l_z} = n\frac{EA}{l} \tag{4}$$

where Δl_z is the vertical displacement at the interface connection. F_z is the force required for the vertical displacement Δl_z; and ε is the axial strain of the bolt, i.e., $\varepsilon = \Delta l_z/l$.

The elastic connection stiffness of S_{Ry} refers to the bending moment required to rotate around the y-axis to produce a unit angle. The corresponding bending moment for generating angle θ is

$$M_O = n(F_x L_z + F_z L_x) \tag{5}$$

$$S_{Ry} = n\frac{F_x L_z + F_z L_x}{\theta} \tag{6}$$

$$\theta = \frac{\Delta l_z}{L_x} \tag{7}$$

$$\Delta l_x = \Delta l_z \tan\theta \tag{8}$$

where Δl_z is the unit elongation of the bolt within the elastic range, i.e., $\Delta l_z = 1$.

Calculated with Eq. (1) to Eq. (8), the parameter of bolts and elastic connection stiffness are summarized in Tabs. 1 and 2.

Tab. 1 Bolt parameters

E/GPa	G/GPa	A/mm^2	l/mm	n
206	79	314	400	13

Tab. 2 Elastic connection stiffness

E_A/MN	G_A/ MN	S_{Dx}/ (MN·m^{-1})	S_{Dz}/ (GN·m^{-1})	S_{Ry}/ (GN·m·rad^{-1})
64.7	24.8	805	2.10	8.41

1.4 Modeling of the pedestrian load

According to the German footbridge design guide EN03[11] and British BS 5400-2 specification[12], structural acceleration limits under different load conditions could be adopted as the comfort evaluation index. In this study, the comfort assessment of the bridge under a single-person moving load (Case 1) and group-pedestrian load (Case 2) was performed by the limit specified in the British BS 5400-2 specification[12]. Meanwhile, the evaluation framework under a high-density crowd (Case 3) was checked using the limit value specified in the German footbridge design Guide EN03 specification[11].

For Case 1, according to the British BS 5400-2[12] specification, when the vertical fundamental frequency of the structure is $1.5\ \text{Hz} \leqslant f_0 \leqslant 5\ \text{Hz}$, the calculation formula of the single-person dynamic load could be expressed as follows:

$$F = \alpha_1 G\sin(2\pi f_0 t) \tag{9}$$

$$v_t = 0.9 f_0 \tag{10}$$

where v_t is the walking speed of pedestrians along the bridge direction; f_0 is the vertical fundamental frequency of the bridge; t is the time of the walking load; G is the gravity of the pedestrian; and dynamic load coefficient $\alpha_1 = 0.257$[12].

For Case 2, pedestrians tend to walk at the same frequency when crossing the bridge at roughly the same velocity. Therefore, the walking-force loading effect of a group of pedestrians F_p can be calculated by multiplying the first-order harmonic component of the walking-force load of a single person by the number of pedestrians in the group:

$$F_p = \alpha_1 G \sin(2\pi f_0 t) n_F \quad (11)$$

where n_F is the number of pedestrians in the group.

For Case 3, when the pedestrian density on the bridge deck exceeds 1.0 person/m^2, pedestrians cannot walk in accordance with their habitual will due to the spacing limitation, and there is a law of the same pace frequency and inconsistent phase between pedestrians[15]. The German specification EN03[11] regards the vertical pedestrian load as a uniformly distributed harmonic load and proposes the expression for calculating the load concentration as follows:

$$p(t) = P\cos(2\pi f_s t) n' \psi \quad (12)$$

$$n' = 1.85\sqrt{n_F} \quad (13)$$

where n' is the equivalent number of simultaneous walkers of n_F freely walking pedestrians; P is the amplitude of the first-order load, and the vertical load P is set as 0.28 kN; $P\cos(2\pi f_s t)$ is the single simple harmonic dynamic load; and ψ is the reduction coefficient of the difference between the natural vibration frequency of the structure and the pedestrian frequency[11].

1.5 Modeling of the traffic load

The influence of the traffic load on structures is mainly due to the vertical pressure generated by the static load of vehicles and the vibration induced by the impact load on the ground during vehicle travel. This phenomenon will lead to a sense of uneasiness while pedestrians walk on bridges[16-18].

As shown in Fig. 5(a), according to the Ref. [19], vehicle loads transferring to the pile foundation should be converted into a dynamic active earth pressure caused by the vertical load of an equally distributed soil layer, and it can be calculated as follows:

$$E_a = \gamma H B K_a \quad (14)$$

where E_a is the active earth pressure; K_a is Rankine's active earth pressure coefficient; γ is the average weight of the earth; and H is the length of the pile foundation. B and h are the calculated width of the pile foundation under the action of the lateral soil pressure and the thickness of the equally distributed soil layer, respectively[19].

As shown in Fig. 5(b), it is assumed that vehicles pass through the pile cap at an identical speed, and the frequency of the load action is expressed as follows:

$$f = \frac{1}{T} = \frac{v}{S} \quad (15)$$

where S is the range of the road where a traveling vehicle can transfer load within this area; v is the speed of the vehicle.

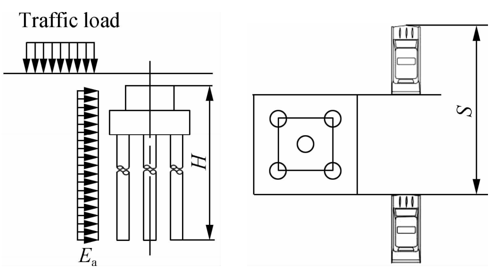

(a) (b)

Fig. 5 Determination of the vehicle load action. (a) Chart of the load action; (b) Schematic chart of the vehicle travel cycle

1.6 Model verification

To verify the accuracy of the FE model, seven measuring points, C1-C7, were arranged on the main span between the two towers of the bridge, as shown in Fig. 6. The natural vibration frequency and the structural response of the pedestrian cable-stayed bridge under the vehicle load were measured with acceleration sensors. Meanwhile, the FE model established in Section 1.2 was used for the numerical calculation, and the numerical results were compared with the collected data.

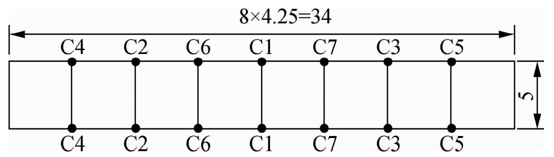

Fig. 6 Layout of the measurement points of the main span of the pedestrian overpass(unit: m)

1.6.1 Natural vibration frequency

After processing the collected data, the measured vibration mode of the bridge is shown in Fig. 7. The first three vibration modes of the structure are the first-order vertical mode, first-order transverse mode, and second-order vertical mode. The corresponding vibration modes in the FE calculation are shown in Fig. 8. Tab. 3 shows the measured and numerical calculation results of the natural vibration frequency of the prefabricated assembled bridge. Apparently, the difference between the collected data and FE calculation results is all within 4%, which means that the FE model can be used to analyze the vibration response of the structure.

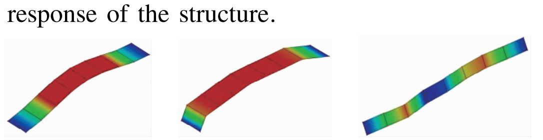

(a) (b) (c)

Fig. 7 Comparisons of the measured structural modes. (a) First-order vertical mode; (b) First-order transverse mode; (c) Second-order vertical mode

(a) (b) (c)

Fig. 8 Comparisons of the FEM structural modes. (a) First-order vertical mode; (b) First-order transverse mode; (c) Second-order vertical mode

Tab. 3 Comparisons between the calculated and measured results

Vibration mode	Frequency/Hz		Difference/
	Measured	FEM	%
First-order vertical mode	1.758	1.771	0.74
First-order transverse mode	3.083	3.206	3.99
Second-order vertical mode	3.455	3.565	3.18

1.6.2 Structural response under the traffic load

The vibration response of the bridge structure was collected during the peak traffic period from 12:00 to 12:15. The measured structural response is shown as the solid line in Fig. 9. When heavy trucks pass under the bridge, the structure acceleration greatly fluctuates, and the maximum peak acceleration reaches 0.101 m/s^2. Comparatively, the car-induced structure response is small, and the maximum peak acceleration is only 0.016 mm/s^2.

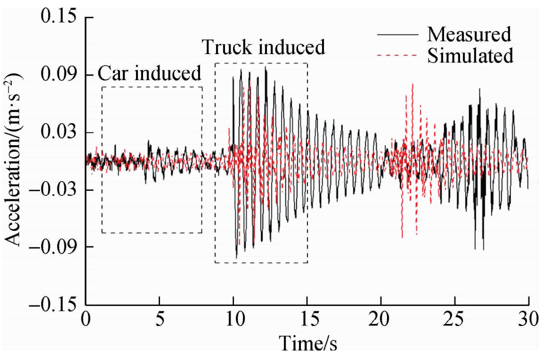

Fig. 9 Structural response comparison

According to the calculation method of the active earth pressure given in Section 1.4, dynamic time-history loads were applied to nodes belonging to the pile foundation in the FE model. The trigonometric function was adopted for modeling heavy trucks and cars. The peak value of the trigonometric function is the active earth pressure calculated in Section 1.4, and the loading period T is the time required for the vehicle to completely pass through the bearing platform. When modeling the traffic load, the heavy truck loading was applied once after the vehicle load was applied every 15 times. The calculated structural response is shown in the dotted line in Fig. 9.

As shown in Fig. 9, the calculated maximum acceleration is 0.015 m/s^2 when the car passes, and the difference with the measured value is approximately 6.7%. However, when the large truck passes, the calculated maximum acceleration is 0.085 m/s^2, which is different from the measured value. The difference of 18.8% is mainly due to the simplification of the vehicle load in the calculation model, and the influence of the vehicle load of other lanes on the structural response is not considered. In general, the numerical structural response agrees well with the overall trend of the measured structural response. The method proposed in this paper can predict the acceleration response of the structure when the vehicle load passes under the bridge, and it can be used to analyze the effect of the vehicle load on the comfort of the pedestrian bridge.

2 Comfort Evaluation

Based on the above analysis results, although bolts were used to connect the adjacent segments, they had a negligible influence on the natural vibration frequency and vibration mode of the structure. Therefore, the existing evaluation method for the comfort assessment of the cast-in-place bridge was adopted in this study to evaluate the prefabricated assembling structure.

2.1 Structural comfort under the pedestrian load

For Case 1, Eq. (9) shows that the single-person dynamic load can be modeled with a sine function of time t. The walking frequency of pedestrians is 1.8 Hz. To make the walking load continuous in time, the length of the beam elements adopted to model the bridge girders in the FE model was set equal to the walking length of the two walking cycles. Pedestrian moving loads were applied to the nodes of beams at two periodic intervals from left to right. The structural damping ratio was set as 2%. The time-history curve of the acceleration at the mid-span position under the load is shown in Fig. 10(a). In the figure, the maximum response of the structure is 0.029 m/s^2.

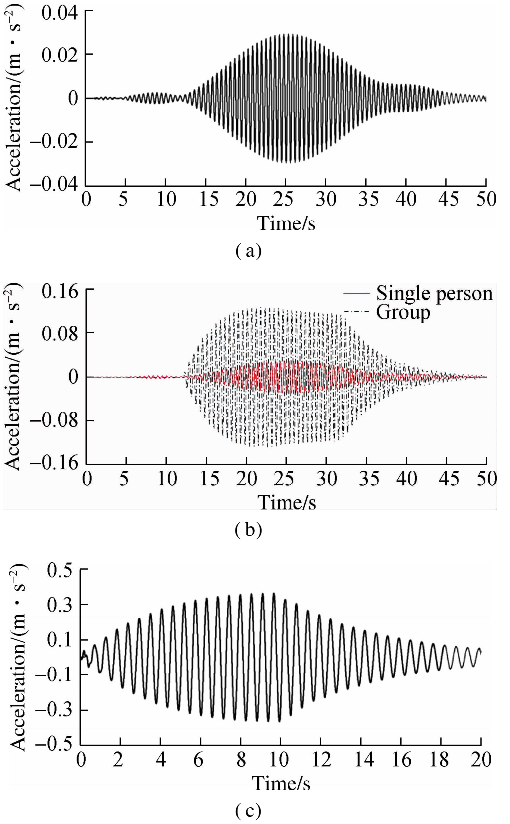

Fig. 10 Pedestrian load span acceleration time-history curve. (a) Single moving load; (b) Group companion load; (c) High-density crowd stepping load

For Case 2, to accurately simulate the synchronous state, a group of pedestrian stepping loads was applied to the amplitude of the first-order mode, and the stepping frequency was set at 1.8 Hz. The acceleration time-history curve of nodes in the mid-span, induced by four-person stepping synchronously and single-person stepping, respectively, is shown in Fig. 10(b). The maximum value of the peak acceleration of the structure is 0.128 m/s^2, which is about four times the maximum response of the single-person moving load.

For Case 3, under this condition, the pedestrian density limit of extremely heavy traffic is 1.5 person/m^2. The maximum number of people on the bridge n_F is 405, and the equivalent number of simultaneous walkers n' is 37. According to the EN03 specification, when the first-order vertical natural vibration frequency of the structure is between 1.7 and 2.1 Hz, the reduction coefficient ψ is 1.0[11]. The pedestrian walking frequency is also 1.8 Hz. The time-history curve of the structural acceleration is shown in Fig. 10(c), and the maximum response acceleration of the structure is 0.364 m/s^2.

The mid-span maximum acceleration response under Cases 1 to 3 is summarized in Tab. 4. In Tab. 4, the peak acceleration of the structure under all working conditions is smaller than the limit value of the reference guidelines.

Tab. 4 Pedestrian comfort check

Case No.	Peak acceleration/ $(m \cdot s^{-2})$	Limited value in Guidelines$(m \cdot s^{-2})$	Comfort evaluation
1	0.029	0.665	Satisfaction
2	0.128	0.665	Satisfaction
3	0.364	0.500	Satisfaction

2.2 Structural comfort under the traffic load

The coupling effect of the pedestrian load and vehicle load on the dynamic performance of the structure was considered in this study[20]. The crowd load stipulated in the Technical Code for Urban Pedestrian Bridges and Pedestrian Tunnels was used to simulate the dense pedestrians, and the quasi-permanent coefficient of the crowd load is 0.4. The first three natural vibration frequencies of the structure with and without the pedestrian load were calculated and are summarized in Tab. 5.

Tab. 5 Effect of the crowd load on the structural vibration frequency

Vibration mode	Frequency/Hz		Difference/%
	Without pedestrian load	With pedestrian load	
First-order vertical mode	1.771	1.722	2.28
First-order transverse mode	3.206	3.140	2.01
Second-order vertical mode	3.565	3.485	2.24

As shown in Tab. 5, the introduction of the crowd load has little influence on the first three-order natural vibration frequencies of the structure. Therefore, the influence of the crowd load can be ignored, and the comfort level of the pedestrian bridge can be directly evaluated according to the peak acceleration of the traffic load. According to the analysis and calculation in Section 1.6, the vertical peak acceleration of the bridge under the vehicle load is 0.085 m/s^2, which is close to the action effect of the pedestrian load in Case 2, indicating that the vehicle load has a certain influence on the vibration of the structure. Compared with the structural acceleration limit of $0.5\sqrt{f_0}$ (0.665 m/s^2) stipulated in the British BS 5400-2 specification[12], the structural comfort meets the requirements.

3 Conclusions

1) The connection between adjacent segments of the prefabricated bridge decks was modeled with the elastic connection in three orthogonal directions, and the calculation method of the stiffness of the elastic connection was presented. Taking the influence of the joint between adjacent segments into consideration, the comfort of the prefabricated and assembled cable-stayed pedestrian bridge was evaluated, and the results demonstrate that the comfort level meets the requirements in different guidelines.

2) The analytical model of the vehicle traffic load was established. Meanwhile, the vehicle traffic load was converted to the active earth pressure in the pile foundation range, and the calculation method of the active earth pressure was presented. Furthermore, the frequency and duration time of the vehicle traffic load were determined.

3) By comparing the measured and numerical values of the natural vibration frequency and structure response, the accuracy of the FE method in predicting the vibration of the bridge was verified. The numerical results clarify that the influence of pedestrian weights on the vibration induced by the vehicle traffic load can be ignored. Moreover, the vehicle traffic load will increase the magnitude of the maximum acceleration and affect the comfort level of bridge structures.

References

[1] Feng P, Wang Z, Jin F, et al. Vibration serviceability assessment of pedestrian bridges based on comfort level[J]. *Journal of Performance of Constructed Facilities*, 2019, **33**: 04019046. DOI: 10.1061/(ASCE)CF.1943-5509.0001316.

[2] Chen Z, Liu G. Pedestrian-induced vibration theory and dynamic design of footbridges[J]. *Engineering Mechanics*, 2009, **26**(S2): 148 − 159. (in Chinese)

[3] Lu P, Zhou Y, Wu Y, et al. Comfort assessment of human-induced vibration of pedestrian bridges based on stevens annoyance rate model[J]. *International Journal of Structure Stability and Dynamics*, 2022, **22**(5): 2250052. DOI: 10.1142/S0219455422500523.

[4] Celik O, Dong C Z, Catbas F N. Investigation of structural response under human-induced excitations using noise-assisted and adaptively transformed multivariate empirical mode decomposition[J]. *Journal of Structural En-*

gineering, 2020, **146**: 4020019. DOI: 10.1061/(ASCE) ST.1943-541X.0002511.

[5] Chen D, Wu J, Yan Q. A novel smartphone-based evaluation system of pedestrian-induced footbridge vibration comfort[J]. *Advances of Structural Engineering*, 2019, **22**: 1685 − 97. DOI: 10.1177/1369433218824906.

[6] Gaawan S M, El-Robaa A S. Pedestrian bridges structure assessment of comfort and impact of human-induced vibration[J]. *Bridge Structures*, 2019, **15**: 3 − 13. DOI: 10.3233/BRS-190148.

[7] Drygala I J, Polak M A, Dulinska J M. Vibration serviceability assessment of GFRP pedestrian bridges[J]. *Engineering Structures*, 2019, **184**: 176 − 85. DOI: 10.1016/j.engstruct.2019.01. 072.

[8] Lievens K, Lombaert G, de Roeck G, et al. Robust design of a TMD for the vibration serviceability of a footbridge[J]. *Engineering Structures*, 2016, **123**: 408 − 18. DOI: 10.1016/j. engstruct.2016.05.028.

[9] Terrill R, Bäumer R, Van Nimmen K, et al. Twin rotor damper for human-induced vibrations of footbridges[J]. *Journal of Structural Engineering*, 2020, **146**: 4020119. DOI: 10.1061/ (ASCE) ST.1943-541X.0002654.

[10] Beijing Municipal Engineering Research Institute. Technical specifications of urban pedestrian overcrossing and underpass: CJJ 69—1995[S]. Beijing: China Architecture Publishing and Media Co. Ltd., 1996. (in Chinese)

[11] Research Found for Coal and Steel. Design of footbridges guideline: EN 03[S]. Aachen, Germany: RFCS, 2008.

[12] British Standards Institution. Steel, concrete and composite bridges: BS 5400-2[S]. London, UK: BSI, 1978.

[13] China Academy of Building Research. Rubber isolation bearing for buildings: JG 118-2000[S]. Beijing: Ministry of Construction of the People's Republic of China, 2020.

[14] Fan W, Sun Y, Sun W, et al. Effects of corrosion and scouring on barge impact fragility of bridge structures considering nonlinear soil-pile interaction[J]. *Journal of Bridge Engineering*, 2021, **26**: 4021058. DOI: 10.1061/(ASCE) BE. 1943-5592.0001757.

[15] Brand M, Sanjayan J G, Sudbury A. Dynamic response of pedestrian bridges for random crowd-loading[J]. *Australian Journal of Civil Engineering*, 2007, **3**: 27 − 38. DOI: 10.1080/14488353.2007.11463918.

[16] Ma F B, Feng D M, Zhang L, et al. Numerical investigation of the vibration performance of elastically supported bridges under a moving vehicle load based on impact factor[J]. *International Journal of Civil Engineering*, 2022, **20**: 1181 − 1196. DOI: 10.1007/s40999-022-00714-3.

[17] Claff D, Williams M S, Blakeborough A. The kinematics and kinetics of pedestrians on a laterally swaying footbridge[J]. *Journal of Sound and Vibration*, 2017, **407**: 286 − 308. DOI: 10.1016/j.jsv.2017.06.036.

[18] Moghimi H, Ronagh H R. Development of a numerical model for bridge-vehicle interaction and human response to traffic-induced vibration[J]. *Engineering Structures*, 2008, **30**: 3808 − 19. DOI: 10.1016/j.engstruct.2008.06.015.

[19] CCCC Highway Consultants Co., Ltd. General code for design of highway bridges and culverts: JTG D60—2015 [S]. Beijing: China Communications Press Co., Ltd., 2015. (in Chinese)

[20] Chen B, Wu D, Xie X, et al. Comfort assessment for a pedestrian passageway suspended under a girder bridge with random traffic flows[J]. *Advances of Structural Engineering*, 2017, **20**: 225 − 34. DOI: 10.1177/1369433216660007.

预制拼装人行斜拉天桥舒适度评价

惠迎新[1,2]　王文炜[3]　刘欣楠[3]

([1]宁夏大学土木与水利工程学院,银川 750021)
([2]宁夏回族自治区道路养护工程技术研究中心,银川 750004)
([3]东南大学交通学院,南京 211189)

摘要:为深入研究预制拼装结构的人致振动特性,采用限制结构加速度响应的方法,对某预制拼装人行斜拉天桥的舒适度进行评价.通过在控制点布设加速度传感器,获得结构在环境激励下的振型、自振频率及阻尼比;根据桥面拼接的弹性连接结构特性,确定相邻节段间的弹性连接刚度;参照国内外相关规范,建立行人和车辆通行荷载分析模型,获得各种荷载工况下的峰值加速度,分析人行天桥的舒适度.结果表明:结构的自振频率和峰值加速度与实测值吻合良好,从而验证了有限元分析模型的有效性;考虑预制拼装对结构刚度的折减可以更真实地反应结构的振动特性,预制拼装结构的舒适度评价指标与整体式结构一致;人群质量对该结构振动频率的影响较小,可以不考虑人群荷载与车辆通行荷载的耦合作用;车辆通行荷载对结构的舒适度产生一定程度的影响.

关键词:预制拼装人行斜拉天桥;弹性连接刚度;车辆通行荷载;振动;舒适度评价
中图分类号:U441.3